The Temperature Field Analysis of the Implantable Medical Device Based on Fluid-Solid Coupling Conjugated Heat Transfer

Xiaoheng Yan[1, 2], Fuyu Ling[2], Weihua Chen[2, *], and Mingchen Cai[2]

Abstract—When an implantable medical device is in radio energy transmission, due to eddy current effect, the temperature of the device will rise, causing a safety risk. In order to study the distribution law of its temperature field, this paper adopts the analysis method of electromagnetic-thermal-fluid-solid multi-physics coupling, and establishes a two-dimensional transient equivalent model of an implantable medical device radio energy transmission system, adopting the analysis method of the electromagnetic-thermal-fluid-solid multi-field full coupling. Among these, electromagnetic heat is applied as the heat source, considering the influence of factors, such as heat conduction and convection. By means of simulated calculation, this paper acquired one-dimensional, two-dimensional and three-dimensional images ,whose temperature and efficiency changed with frequency. Moreover, their distribution laws are also obtained. In order to verify the correctness of the simulation, this paper conducts infrared temperature measurement experiments to prove the rationality of the analysis through comparing the simulation results. The research findings of this paper can provide a basis for the design of a radio energy transmission system for an implantable medical device, improve the safety of implantable medical devices, and reduce the occurrence of medical accidents. Meanwhile, it has certain reference value to the clinical application of implantable medical devices.

1. INTRODUCTION

Currently, implantable medical devices become a widely-applied treatment [1]. However, implantable medical devices utilize batteries as a power source, which severely limits their service lives, and changing the batteries results in second pain to the patients. Therefore, it is of practical significance to transmit radio energy to implantable medical devices.

Since the first realization of radio energy transmission for implantable medical devices in the 1960s, researchers have conducted in-depth researches on many aspects, including efficiency optimization and bio-safety, etc. In terms of transmission efficiency, [2] established the equivalent circuit model of magnetic coupling energy transmission in metal-containing medium, proposed the system design method with receiving efficiency as the optimization target, and applied it in the development of rechargeable computer pacemaker. However, the established circuit model could not truly simulate the complex environment of human body. Ref. [3] considered the influence of load on the input impedance of power recovery circuit, proposed a non-resonant method for adaptive impedance tuning, designed a small-sized ultrasonic receiver to efficiently supply power to the implanted medical device, and increased the overall implantation efficiency. However, it did not consider problems that after the system had worked for a certain period of time, the heating of metal medium would lead to the obstruction of energy propagation, the instability of the system, and the reduction of efficiency. Ref. [4] put forward a new radio transmission technology based on the optimal resonant load transformation, which greatly

improved transmission efficiency by adding only one inductor component chip. However, it adopted the transmission frequency of 13.56 MHz without considering the shielding effect of metal. Ref. [5] designed a new clamping radio energy transmission system. The key of this design was to adopt a unique sandwich topology in the transmitter and receiver coils, which improved the transmission power as well as the flexibility of the charging system effectively. However, it did not consider the shielding effect of the receiving casing. In terms of security, [6, 7] were from the perspective of biological electromagnetic radiation safety, applied time domain finite difference method, and conducted analysis on the human body's specific absorption rate SAR distribution in an electromagnetic environment, providing a theory for the calculation and analysis of electromagnetic safety. However, when modeling, they did not consider the shielding effect of the receiving casing of an implantable medical device; Ref. [8] proposed a design of inductive coupling circuit between an in vitro loop antenna and a three-dimensional implantable antenna. Verified by modeling and experiment, the proposed 3D implantable antenna was suitable for a small radiotactic brain implantable medical device, which could satisfy the distribution of SAR and temperature in human head model. However, the induction coupling method required a short distance between the transmitting coil and receiving coil. Moreover, accurate alignment was necessary for efficient transmission. The above requirements limited the application of the implantable device to a certain extent; based on the basic principle of magneto-coupled resonance, Ref. [9] designed a detailed optimization method for the free-floating implantable device. Moreover, it established the real finite element simulation model of head tissue by HFSS simulation software and explored the design strategy and safety problems, such as coil segmentation and specific absorptivity limit. Ref. [10] designed a transcutaneous transformer with high coupling and small size. The axial displacement of the coil was 5 mm, and the coupling coefficient was still as high as 0.8, indicating that the displacement greatly improves the transmission efficiency. However, it did not overcome some unfavorable factors, such as the short transmission distance of inductive coupling. Ref. [11] developed a transcutaneous energy transmission system and analyzed its temperature characteristics by means of multi-physics coupling. It found that when the power supply was satisfied, the temperature rise was within the range of human body regulation. However, it did not analyze the biological compatibility of the system and safety factors (such as electromagnetic radiation). Ref. [12] implanted a high-power transcutaneous transformer into the sheep. By changing the power, it observed the temperature distribution of transmitting and receiving coils and developed the transcutaneous energy transfer system. The details of this system were as follows: the transmission power was 7 W; the efficiency was 80.5%; the temperature rise of the receiving coil was 2°C. However, it did not consider the eddy current heat of the receiving end casing.

Eddy current has great potential in industrial field. For instance, in nondestructive testing [13, 14], in contrast to other methods, the application of eddy current imaging has the characteristics of thrift, simplicity, fast detection, high efficiency, realizing automation easily, etc. [15–17]. Eddy current brake made of eddy current is also widely applied in vehicle auxiliary braking systems, vehicle suspension systems, space docking mechanism, braking of high-speed train, transmission systems, structural vibration suppression, energy absorption systems, and other engineering fields [18–21].

In general, there are two main methods to research on the radio energy transmission system of implantable medical devices: the equivalent analysis method of circuit and the physical field coupling analysis method. However, in the complex environment of human body, it is difficult to accurately simulate the real environment of human body by applying the empirical formula of circuit analysis. The coupling relationship between solid field and other fields is always ignored or simplified by the constant heat transfer coefficient in most multi-physics coupling analysis methods. Meanwhile, in the process of modeling, most of them ignore the shielding effect of the receiving casing, which cannot truly simulate the radio transmission system of the implantable medical device. From the perspective of the electromagnetic-thermal-fluid-solid multi-physical field coupling field, this paper simulates the complex environment of human body and establishes the real model with receiving end casing. Simulated calculation is conducted on the temperature field distribution of the implantable medical device radio energy transmission system. Through the comparison with the experimental data, the effectiveness and accuracy of the method are verified. Studying the distribution of the temperature field of a radio energy transmission system of an implantable medical device can accomplish the prediction for the temperature and position of the local hot spot. In this way, it can be applied to guide the structural design of the implantable medical device radio energy transmission system, improve the thermal performance and

service life of the device, improve the operation state of the device, and reduce the occurrence of accidents.

2. THEORETICAL ANALYSIS OF THE SYSTEM

2.1. Working Principle and Circuit Model

An implantable medical device radio energy transmission system is mainly composed of a transmitting coil, a receiving coil, and a titanium alloy metal casing. Generally, the coil adopts a primary energy coil and a secondary energy receiving coil arranged in a plane spiral. When transmitting radio energy to an implantable medical device, due to the eddy current effect caused by the AC electromagnetic field, the metal casing will dissipate part of the energy in the form of heat. Simultaneously, the eddy current will excite an induced magnetic field. Namely, the metal casing shows the effect of inductance and resistance at the same time. The equivalent circuit model of magnetic coupling energy transmission of implantable medical device is shown in Fig. 1 [2].

In Fig. 1, L_1 is the transmitting coil inductance; R_1 is the transmitting coil resistance; L_2 is the receiving coil inductance; R_2 is the receiving coil resistance; L_3 is the metal casing equivalent inductance; R_3 is the metal casing equivalent resistance; the coupling degrees among three of them are represented by M_{12}, M_{13}, and M_{23}, respectively.
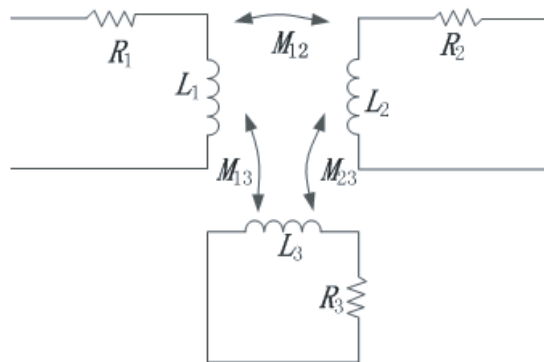
Figure 1. Equivalent circuit model of implantable medical device radio energy transmission system.

2.2. The Magnetic Field's Governing Equation

The eddy current effect from the metal shell of the implanted device is the main heat source. Among these, the eddy current loss is closely related to the magnetic flux density distribution. Therefore, the magnetic field distribution of the metal shell needs to be solved first. According to the Maxwell's equation, the electromagnetic field governing equation is as follows [22]:

$$\nabla \times \frac{1}{\mu} (\nabla \times A) = J - \sigma \frac{\partial A}{\partial t} \tag{1}$$

where $\mathbf{A}$ is the magnetic vector potential; $\mathbf{J}$ is the current density; and σ is the conductivity.

2.3. The Conjugated Heat Transfer Governing Equation

In an alternating magnetic field, the titanium alloy metal casing produces significant eddy current losses, which will be converted into heat. Moreover, the generated heat relies on the wall of the casing to form a heat exchange with the air, causing the hot floating flow of the air. This complex flow-solid-thermal multiphysics coupling process can be described by a conjugated heat transfer control equation, which covers solid heat transfer and fluid heat transfer processes. The solid heat transfer is dominated by conduction, while fluid heat transfer is dominated by convection. On the basis of achieving thermal equilibrium, it is necessary to set the boundary conditions and obtain the temperature field analysis

accurately. Under an alternating magnetic field, the eddy current generated by the metal casing is as follows:

$$q_v = \rho_1 |J|^2 \tag{2}$$

where $\mathbf{q}_v$ is the strength of the heat source, and ρ_1 is the resistivity of the metal casing.

In an isotropic material, if the physical quantity performance parameter is constant, then the Fourier thermal differential equation in a Cartesian coordinate system is as follows [23]:

$$\frac{\partial^2 T}{\partial x^2} + \frac{\partial T}{\partial y^2} + \frac{q_v}{k} = \rho \frac{c}{k} \frac{\partial T}{\partial t} \tag{3}$$

where $\mathbf{T}$ is the temperature; ρ is the density of the material; k is the heat transfer coefficient; and c is the specific heat capacity of the metal shell material.

In the calculation of the heat-flow coupled field, factors, such as heat conduction and convection heat transfer, are considered. Heat conduction is a heat transfer phenomenon in the medium without macroscopic motion, which can occur in solids, liquids, and gases. The governing equation [23, 24] is as follows:

$$\rho c \frac{\partial T}{\partial t} = \tau \left(\frac{\partial^2 T}{\partial x^2} + \frac{\partial^2 T}{\partial y^2} \right) + Q \tag{4}$$

where x and y are coordinate values; τ is the thermal conductivity; t is the time; $\mathbf{Q}$ is the heating power per unit volume.

The fluid's heat-transferring process mainly includes three contributions. According to the thermal properties of fluid and flow pattern, it may be mainly convective and conductive heat transfer. The viscous effect of fluid flow can cause fluid heating, which is usually ignored. However, it should be considered in the case of fast flowing viscous fluids. If the fluid's density varies according to temperature, a pressure contribution should be added to the heat transfer equation. In order to accurately explain the coupling relationship among the above three heat transfer contributions, the following transient heat transfer equation is obtained [25].

$$\rho_i C_p \frac{\partial T}{\partial t} + \rho_i C_p u \cdot \nabla T = \alpha_p T \left(\frac{\partial pA}{\partial t} + u \cdot \nabla p_A \right) + \tau_i : S + \nabla \cdot (k \nabla T) + Q_s \tag{5}$$

where C_p is the constant pressure heat capacity; g is the gravitational acceleration; k is the thermal conductivity; p_A is the absolute pressure; q is the heat flux; Q_i is the heat source; S is the strain rate tensor; u is the velocity; α_p is the thermal expansion coefficient; ∇T is the characteristic temperature difference; ρ_i is the fluid density; τ_i is the viscous stress tensor.

The device is filled with air, so the fluid flows freely within internal cavity. The shell is maintained at high temperature caused by eddy current loss, and the external boundaries are opened. The temperature differential produces the density variation that drives the buoyant flow. The compressible Navier-Stokes equation contains a buoyancy term on the right-hand side to account for the lifting force due to thermal expansion that causes density variations [26]:

$$\rho(\mathbf{u} \cdot \nabla)\mathbf{u} = -\nabla p + \nabla \cdot \mu \left(\nabla \mathbf{u} + (\nabla \mathbf{u})^T \right) - \frac{2}{3}\mu(\nabla \cdot \mathbf{u}) = \rho \mathbf{g} \tag{6}$$

where the dependent variables for flow are the fluid velocity vector $\mathbf{u}$ and pressure p; constant $\mathbf{g}$ denotes the gravitational acceleration; ρ gives the temperature dependent density; μ is the temperature-dependent dynamic viscosity. Because the model only contains information about the pressure gradient, it estimates the pressure field up to a constant. To define this constant, we arbitrarily fix the pressure at a point. No slip boundary conditions are applied on all boundaries. The no slip condition results in zero velocity at the wall but does not set any constraint on p. At steady-state, the heat balance for a fluid is reduced to the following equation [26]:

$$\rho C_p \mathbf{u} \cdot \nabla T - \nabla \cdot (k \nabla T) = 0 \tag{7}$$

where T represents the temperature; k denotes the thermal conductivity; C_p is the specific heat capacity of the fluid.

3. SIMULATION ANALYSIS

3.1. Establishment of the Model

Currently, there are many kinds of implantable devices, whose size, power, and position are varied. The purpose of this paper is to research the distribution of the eddy current heat in the charging process of an implantable medical device. The simulation model is mainly aimed at brain pacemaker and cardiac pacemaker. The implantable medical device radio energy transmission system is mainly composed of a driving circuit module, a transmitting coil, a receiving coil, and a metal casing. Among these, the transmitting coil is external to the body, and the receiving coil together with the implantable medical device is implanted into the body. The schematic diagram is shown in Fig. 2. In the energy transmission, the electromagnetic-thermal-fluid solid physical process consists of a coupling of a drive circuit and an electromagnetic field, a coupling of electromagnetic and solid heat transfer, and a coupling of solid heat transfer and non-isothermal flow. In this paper, COMSOL's built-in electromagnetic field, solid heat transfer, and non-isothermal flow modules are utilized to describe the implantable medical device radio energy transmission system so as to conduct more detailed simulated research in an accurate way. Since the main purpose of this paper is to study the law of temperature rise caused by the eddy current effect in wireless power supply of implantable medical equipment, the initial temperature requirement is relatively low, and the main factor affecting the temperature rise is the material of the outer casing. On this basis, the following assumptions are made in order to ensure the rationality of the simulation and reduce the computational memory.

1) The metal casing of the implanted device is replaced by a regular rectangle, ignoring the effect of the shape on the simulation results.

2) Air replaces human tissue for coupling analysis [27].

3) The initial temperature is given as room temperature $20°C$.

4) The effect of Lorentz force on the fluid field is ignored.

5) The change in thermal conductivity of titanium alloys with temperature is ignored.

In summary, a two-dimensional axisymmetric geometric model describing a radio energy transmission system for an implantable medical device can be established, which is shown in Fig. 3.
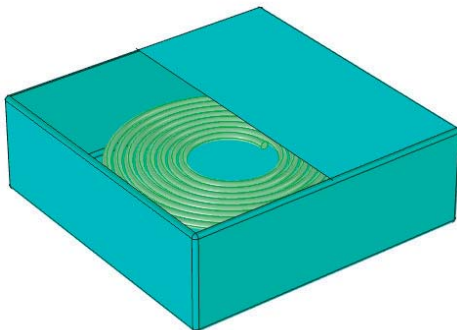
Figure 2. Schematic diagram of the receiving end of the implantable medical device.
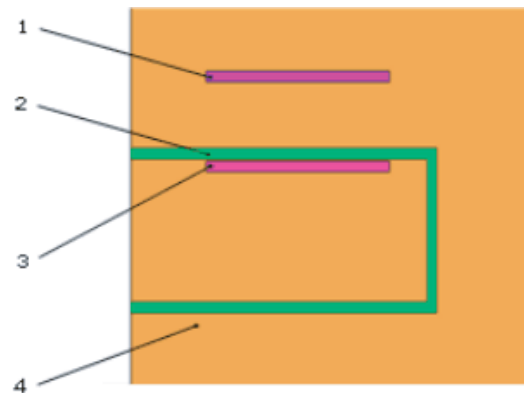
Figure 3. Two-dimensional axisymmetric geometric model.

According to Fig. 3, in the geometric model, 1 represents the primary transmitting coil; 2 represents the titanium alloy metal casing; 3 represents the secondary receiving coil; and 4 represents the multi-physics solving domain working medium.

The boundary condition setting is as follows: Two-dimensional axisymmetric model is adopted; initial temperature setting is $T_0 = 20°C$; heat source is derived from eddy current loss caused by induced current; fluid wall surface is without slip boundary condition.

3.2. Analysis of Simulation Result

According to [28–30], we take into account the following factors simultaneously: the general implanted medical equipment volume cannot be too large; the human skin thickness is generally 8–12 mm; the load is generally 2–200 Ω. In consideration of many safety factors, such as human body electromagnetic radiation, we set the operating frequency to 70–700 kHz. The dimensions of the coil and metal casing of the implantable medical device radio energy transmission system described in this paper, as well as other parameters required in the calculation process, are shown in Table 1. A sinusoidal excitation with the amplitude of 12 V is applied at the transmitting end, and the load is 30 Ω. The following simulation results are obtained.

Table 1. Calculation parameter.

Attributes	Air	Coil	shell
Outer Diameter (mm)		22.5	
the Inside Diameter of (mm)		5	
Wire Diameter (mm)		0.1	
Shell (mm)			$70 * 70 * 0.5$
Number of Turns		16	
Relative Permeability	1	1	1
Thermal Conductivity (W/(m·k))	K(T)	400	7.5
Relative Permittivity		1	
Conductivity (S/m)	0		$2.38 * 106$
Constant Voltage Capacitor (J/(kg·K))	CP(T)	385	710

1) Efficiency Analysis

The power distribution curve at the resonant frequency of 100 kHz and 700 kHz is shown in Fig. 4 when the distance between the transmitting coil and the implanted device is constant, and the distance between the receiving coil and the metal casing is 0.01 mm.

As we can see from Fig. 4, for the implantable medical device radio energy transmission system, the higher the frequency is, the more serious the shielding effect is, and the smaller the receiving power is. Even if resonance occurs, and the transmission is performed at a frequency of 700 kHz, the power is also very small (about 1 mW), which can only meet the requirements of small power devices, such as pacemakers and nerve stimulators. To increase the power of the receiving coil, we can increase the input voltage of the transmitting end. However, we should consider that the application object is the human body. If the input voltage is too high, it will pose a threat to human safety.

2) Analysis of the Flow field

Figure 5 reveals the velocity field distribution near the radio energy transmission system of an implantable medical device after charging for 10 s and 1 h at a resonant frequency of 300 kHz. It can be seen from Fig. 5(a) that corresponding to the temperature field distribution, the velocity distribution also forms a certain internal flow around the high temperature region and low temperature wall surface. Due to the uneven heating, the air forms a flow around the titanium alloy shell and flows out in a radial direction. It can be seen from Fig. 5(b) that the outflow direction of the air is converted into the upper side outflow. This is because the heat buoyancy effect of the air, due to the heat exchange process with the outside world, is more significant than that of the air gravity. Therefore, the air flows out through the upper side after 1 hour, which is highly consistent with the actual situation.

3) Analysis of the Temperature Field

At a resonant frequency of 300 kHz, it can be seen from Fig. 6(a) and Fig. 6(b) that after the implanted medical device is continuously charged for 0.2 h, the temperature of the metal casing reaches a maximum of 20.5°C, and the temperature is mainly concentrated on the upper surface of the titanium alloy casing, which is increased by 0.5°C in comparison to the initial temperature. The main cause
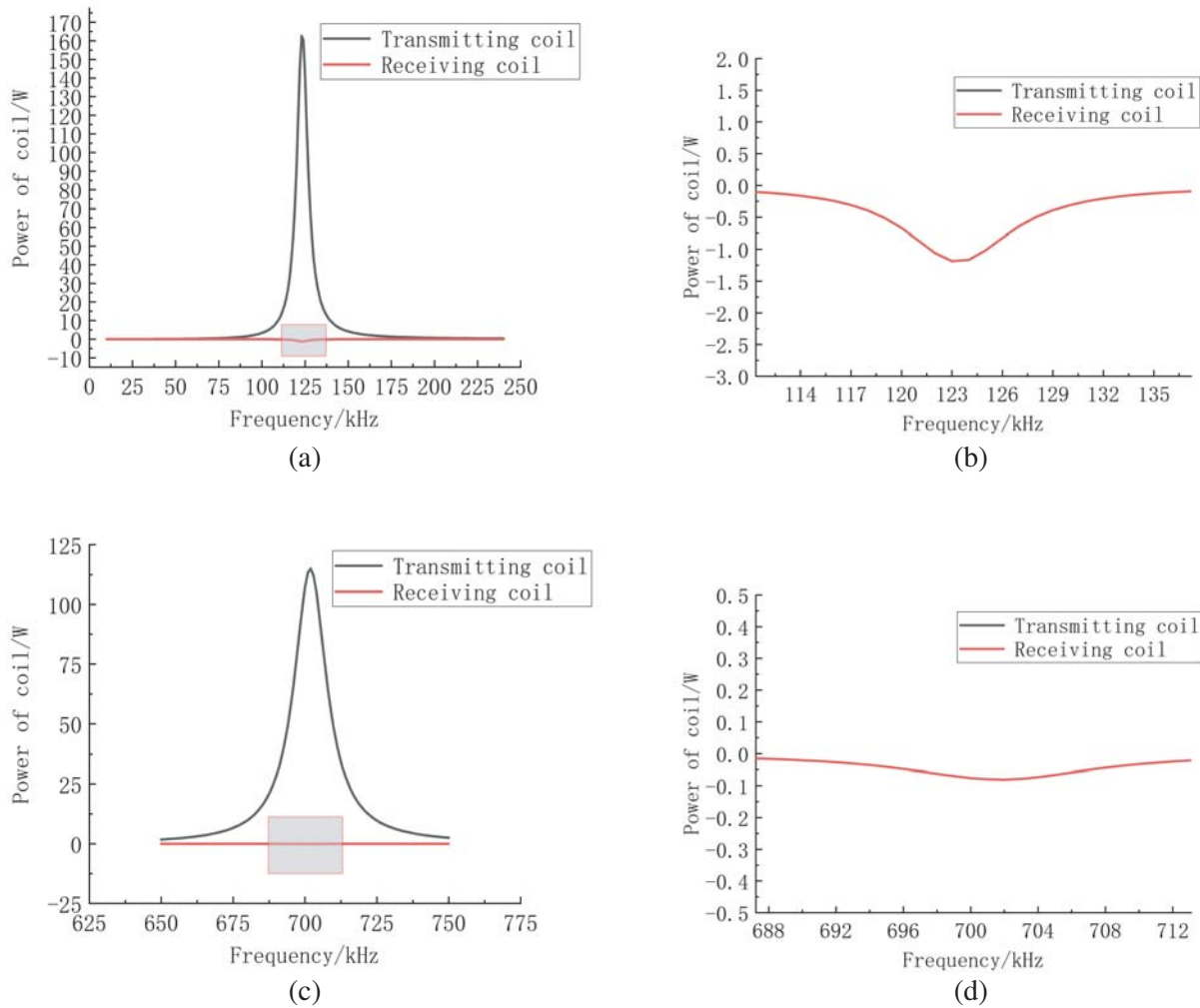
Figure 4. (a) Power curve at resonant frequency 125 kHz; (b) Partial magnification of the resonant frequency at 100 kHz; (c) Power curve at resonant frequency 700 kHz; (d) Partial magnification of the resonant frequency of 700 kHz.

of this phenomenon is the eddy current effect. After 0.6 h, the maximum temperature of the device reaches 21.2°C. In contrast to the initial 0.2 h, the temperature rise gradient decreases significantly. This is mainly because the heat exchange process with the outside air is gradually strengthened, and heat dissipation can be formed relatively quickly.

The local heating of the human body caused by an increase in the temperature of the implanted device will lead to a series of problems, such as neurological dysfunction and protein denaturation. Some people have convulsions at a temperature of 41°C, usually 43°C is defined as the body heat damage temperature. When the implanted device heats up in the human body, the temperature regulation system of the human body begins to function. At this moment, the convective heat dissipation with the external air plays an important role in the perfusion of the human capillaries. The thermal properties of biological tissue are generally defined by the Pennes bioheat transfer equation [31] given by

$$\rho_i c \frac{\partial T}{\partial t} = \nabla \times (k\nabla T) + (\rho_i c)_b \omega_m (T_1 - T_2) + Q_m p(z, t) \qquad (8)$$

where ω is the blood perfusion volume rate per unit volume of tissue; subscript b refers to blood; $p(z, t)$ is the heat per unit volume due to spatial distribution during heating; ω_m is a function of temperature-dependent perfusion temperature. Studies have shown that [31] when the local temperature of the
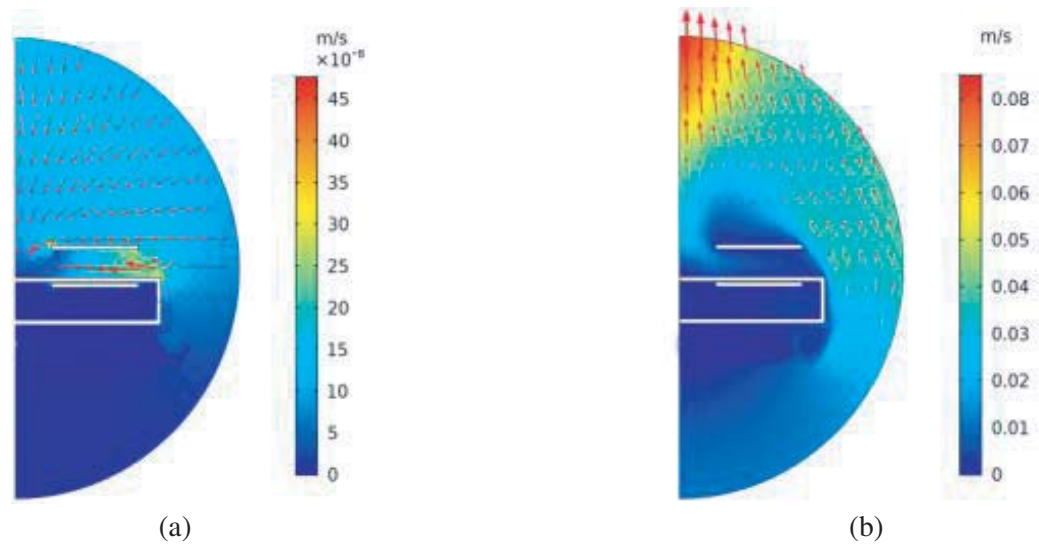
Figure 5. (a) Flow field distribution outside the shell at 10 s; (b) Flow field distribution outside the shell at 1 h.
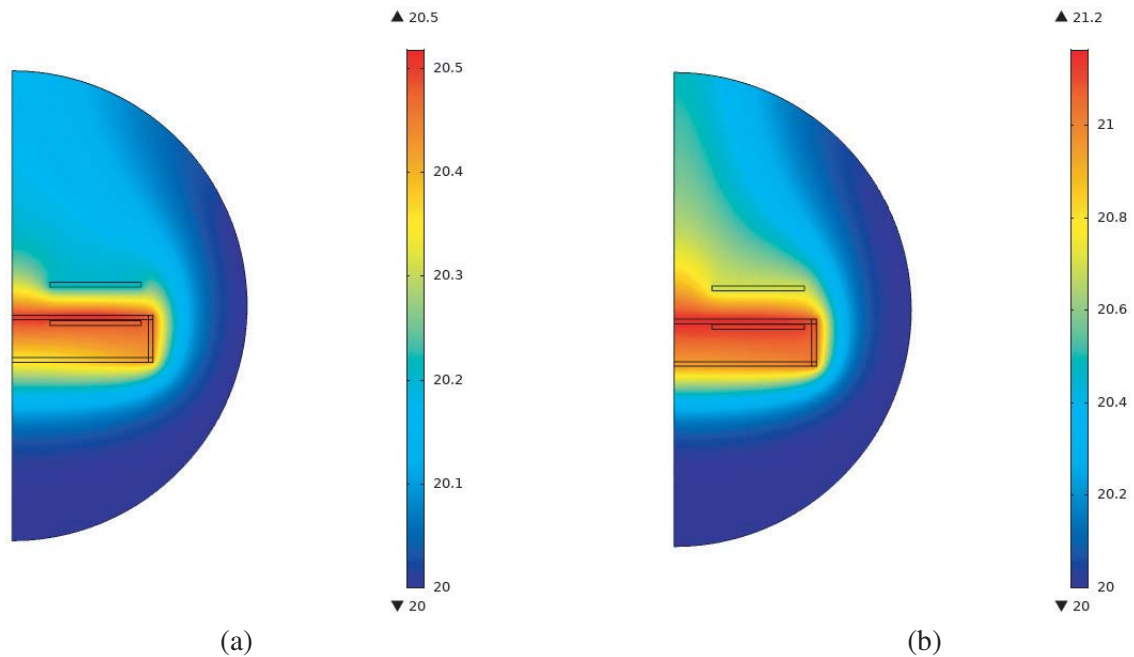

Figure 6. (a) Temperature field distribution of 0.2 h equipment; (b) Temperature field distribution of 0.6 h equipment.

human body increases, due to the body's temperature regulation, blood flow can be increased by 15 times in just a few minutes to 100 ml 100 g min^{-1}.

Therefore, in order to find an optimal operating frequency for the radio energy transmission system of the implantable medical device (i.e., to consider the factors such as efficiency and distance under the premise of ensuring the safety of human body), it is necessary to analyze the temperature rise at different resonant frequencies. We take the highest temperature point $A(-9, -2)$ of the implanted medical device shell and obtain a one-dimensional curve of temperature change relationship at different resonant frequencies through simulation (See Fig. 7).
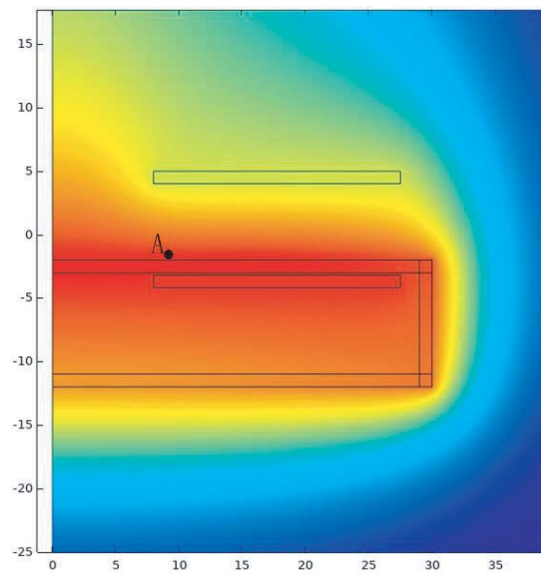
Figure 7. Schematic diagram of the highest temperature point.
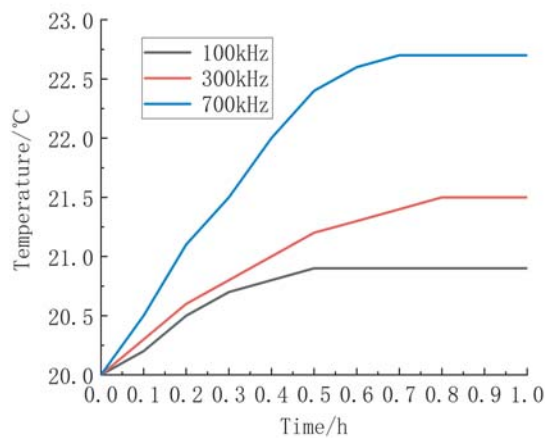
Figure 8. One-dimensional curve of temperature-time relationship of different resonant frequencies.
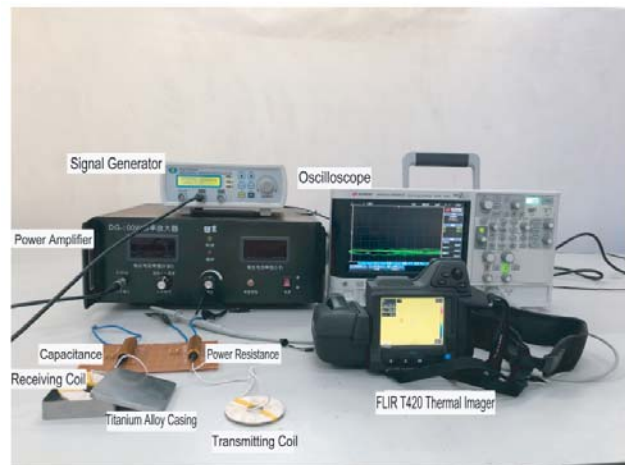
Figure 9. Experimental platform for the implantable medical device radio energy transmission system.

It can be seen from Fig. 8 that for the radio energy transmission system of the implantable medical device, in the case that other parameters are given, the higher the resonance frequency is, the higher the temperature rise is when the distance between the receiving coil and outer casing is constant. When the resonant frequency is 700 kHz, and it is heated continuously for 0.7 h, the temperature will reach a steady state (the maximum temperature is 22.7°C). For the radio energy transmission system, the higher the frequency is, the higher the efficiency is. However, when the system is applied to an implantable medical device, the direction of the emitted magnetic field generated by the eddy current effect is opposite to the direction of the excitation magnetic field generated by the transmitting coil. Namely, the presence of the metal outer casing reduces the magnetic flux at the receiving end. The closer the receiving coil is to the outer casing, the more obvious this kind of effect is. Meanwhile, the temperature rises, causing damage to human tissues.

4. THE EXPERIMENTAL VERIFICATION

4.1. Configuration of the Experimental Platform

In order to verify the rationality of the simulation method, an experimental platform for temperature detection of the implantable medical device radio energy transmission system is established, as shown in Fig. 9. The experimental platform mainly includes: signal generator, oscilloscope, power amplifier, high-precision FLIR T420 thermal imager, titanium alloy casing, transmitting coil, receiving coil, etc. Among these, the signal generator and power amplifying device are applied as power sources in the experimental circuit to provide reliable power for the system. A multi-channel digital oscilloscope, a thermal imager, and the like constitute a measurement circuit for measuring the current, voltage, and temperature distribution of the experimental output. In order to ensure the winding precision of the coil, the multi-strand enameled wire is wound by a fully automatic winding machine, and the center position and direction angle of the coil are determined by means of a mechanical adjustment frame. In consideration of factors, such as biocompatibility and magnetic shielding, the housing of implantable medical devices is generally made of titanium alloy. Therefore, in the test, the subject is made of Ti-6Al-4V material, and a medical titanium alloy casing is produced by 3D printing technology.

4.2. Analysis of Results

To verify the simulation results, we conduct temperature rise experiments at resonance frequencies of 100 kHz, 300 kHz, and 700 kHz, respectively. The effective value of the input voltage, initial temperature, relative humidity and reflection temperature in the experiments are 12 v, 20°C, 50%, and 15°C, respectively. After the implantable medical device is continuously charged for 0.2 h and 0.6 h in the resonant frequency of 300 kHz, the measured surface temperature rise is obtained respectively, as shown in Fig. 10. The temperature curves in different resonance frequency are shown in Fig. 11.
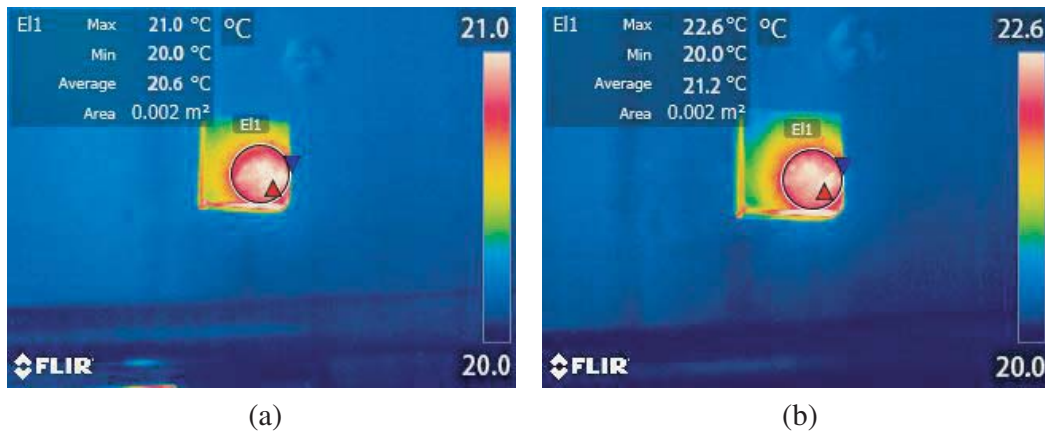
Figure 10. (a) 0.2 h temperature rise measured map; (b) 0.6 h temperature rise measured map infrared thermometry.

By comparing Fig. 6 and Fig. 10, it can be found that the experimental measured temperature is higher than the simulation results, and the maximum difference appears at 0.6 h. Within 1 h of continuous charging, the trend of temperature increase at the highest point on the receiver surface is basically the same, and the temperature is positively correlated with the frequency. From the observation of Fig. 10, we can see that the temperature is mainly concentrated on the upper surface of the receiver casing, and the distribution shape is roughly the same as that of the coil geometry. It can be seen from Fig. 11 that under different resonant frequency lines, the temperature rise in the early stage is faster, and the temperature rise effect is obvious. After the continuous power supply for 0.6 h, the temperature rise speed of the three experimental systems obviously becomes slower. After 0.8 h, it reaches a steady state, and the temperature basically remains unchanged. When the resonant frequency is 700 kHz, the
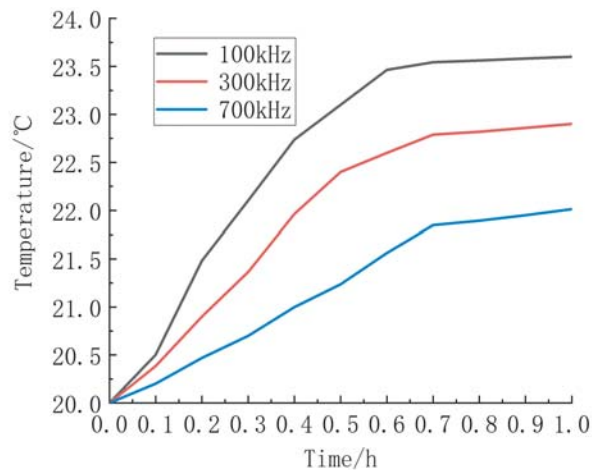
Figure 11. One-dimensional curve of temperature-time relationship of different resonant frequencies.

maximum temperature rise of the experimental system is 23.5°C after continuous charging for 0.7 h. The error with the simulation data is 0.8°C. The primary causes of the error are as follows: the thermal radiation effect of the transmitting and receiving coils on the casing of the implantable medical device is neglected in the simulation calculation, and the heat transfer between the receiving coil and casing of the receiving end is ignored. Another factor is that the thermal effect caused by the presence of SAR is ignored in the multi-physics coupling analysis.

5. CONCLUSIONS

In this paper, a two-dimensional axisymmetric transient equivalent model of an implantable device radio energy transmission system is established to analyze the temperature variation law of the metal shell at the receiving end. The electromagnetic-heat flow-solid multiphysics physics coupling analysis method is utilized to obtain the following conclusions:

1) With regard to the implantable medical devices powered by radio energy transmission, the surface temperature rises due to the eddy current effect, and the maximum temperature is mainly concentrated on the surface of the titanium alloy casing of the implanted device. Furthermore, the temperature rise is positively correlated with the resonant frequency, which is roughly the same as the shape of the coil.

2) Clinically, the thermal safety temperature of the human body is defined as 43°C. Based on the experimental and simulation conclusions of this paper, it can be concluded that under the premise of ensuring human body safety, it is safer to set the frequency of the emission source below 1 MHz and then go on this basis. Consider other factors that affect the transmission of radio energy. On this basis, subsequently, we can consider other factors that affect the transmission of radio.

3) As far as the receiving end is concerned, the higher the frequency is, the more severe the shielding effect of the titanium alloy is. When the resonant frequency is MHz, the power at the receiving end is only mW or less, which can only power for some small power implanted devices, such as nerve stimulators, drug sputum, cochlear implants, cardiac pacemakers, and the like.

4) Through the temperature rise test, the rationality of the electromagnetic-heat flow-solid multi-physics coupling simulation calculation method is verified. The simulation results of the highest temperature point and temperature rise test results are compared and analyzed. The results reveal that the percentage difference is within 8%, which proves the accuracy of the simulation calculation method.

REFERENCES

1. Lovik, R. D., J. P. S. Abraham, and E. M. Parrow, "Surrogate human tissue temperatures resulting from misalignment of antenna and implant during recharging of a neuromodulation device," *Neuromodulation: Technology at the Neural Interface*, Vol. 14, 501–511, 2011.

2. Li, Q., S. Chen, W. Wang, H. Hao, and L. Li, "Optimization of magnetic coupling energy transfer in active implanted systems," *J. Tsinghua Univ.*, Vol. 55, 351–355, 2015.

3. Chang, T. C., M. J. Weber, and M. L. Wang, "Design of tunable ultrasonic receivers for efficient powering of implantable medical devices with reconfigurable power loads," *IEEE Trans. Ultrason. Ferroelectr. Freq. Control*, Vol. 63, 1554–1562, 2016.

4. Xue, R. F., K. W. Cheng, and M. Je, "High-efficiency wireless power transfer for biomedical implants by optimal resonant load transformation," *IEEE Trans. Circuits Syst. I, Reg. Papers*, Vol. 60, 867–874, 2013.

5. Liu, C., C. Jiang, J. Song, et al., "An effective sandwiched wireless power transfer system for charging implantable cardiac pacemaker," *IEEE Transactions on Industrial Electronics*, Vol. 66, No. 5, 4108–4117, 2019.

6. Zhao, J., G. Xu, C. Zhang, et al., "Study on the influence of head-embedded coils on the electromagnetic radiation of human head in magnetically coupled resonant wireless energy transmission system," *Chin. J. Biomed. Eng.*, Vol. 31, 649–654, 2015.

7. Gong, F., Z. Wei, and Y. Cong, "Research on the influence of electromagnetic resonance wireless energy transmission system antenna on the electromagnetic radiation safety of implantable medical equipment," *Chin. J. Biomed Eng.*, Vol. 38, 497–501, 2016.

8. Manoufali, M. and A. Abbosh, "Specific absorption rate and temperature increase for a passive brain implantable medical device using transmission line analysis," *2017 IEEE (APMC)*, 570–572, 2017.

9. Mirbozorgi, S. A., P. Yeon, and M. Ghovanloo, "Robust wireless power transmission to mm-sized free-floating distributed implants," *IEEE Transactions on Biomedical Circuits and Systems*, Vol. 11, No. 3, 692–702, 2017.

10. Ma, J., Q. Yang, and H. Chen, "Transcutaneous energy and information transmission system with optimized transformer parameters for the artificial heart," *IEEE Trans. Appl. Supercond.*, Vol. 20, 798–801, 2010.

11. Ma, J., B. Liu, Y. Li, et al., "Temperature field of transcutaneous transformer for artificial heart," *Journal of Hebei University of Technology*, Vol. 43, 33–36, 2014.

12. Dissanayake, T. D., D. Budgett, P. Hu, et al., "Experimental thermal study of a TET system for implantable biomedical devices," *2008 IEEE Biomedical Circuits and Systems Conference*, 113–116, IEEE, 2008.

13. Versaci, M., "Fuzzy approach and eddy currents NDT/NDE devices in industrial applications," *Electronics Letters*, Vol. 52, No. 11, 943–945, 2016.

14. Megali, G., D. Pellicano, M. Cacciola, S. Calcagno, M. Versaci, and F. C. Morabito, "EC modelling and enhancement signals in CFRP inspection," *Progress In Electromagnetics Research M*, Vol. 14, 45–60, 2010.

15. Harmouche, J., C. Delpha, D. Diallo, et al., "Statistical approach for nondestructive incipient crack detection and characterization using Kullback-Leibler divergence," *IEEE Transactions on Reliability*, Vol. 65, No. 3, 1360–1368, 2016.

16. Larsson, L. and A. Boström, "Integral equation method for evaluation of eddy-current impedance of a rectangular, near surface crack inside a cylindrical hol," *Journal of Nondestructive Evaluation*, Vol. 35, No. 2, 21–31, 2016.

17. Le, M., J. Kim, S. Kim, et al., "Nondestructive evaluation algorithm of fatigue cracks and far-side corrosion around a rivet fastener in multi-layered structures," *Journal of Mechanical Science & Technology*, Vol. 30, No. 9, 4205–4215, 2016.

18. Feng, Y., S. Huang, W. Zhang, et al., "An attempt to improve the braking capacities of eddy current retarder with double-rotor excitation structure," *Electrical Machines and Systems, Busan,*

703–707, 2013.

19. Wang, X. and D. Wang, "Calculation of eddy current loss and thermal analysis for adjustable permanent magnetic coupler," *Electronic & Mechanical Engineering and Information Technology*, 4405–4408, Harbin, 2011.

20. Singh, A. K., "Model development of eddy current brakes for energy absorbing system," *Recent Developments in Control, Automation and Power Engineering*, 382–384, Noida, 2015.

21. Filho, R. F. P., A. O. Salazar, F. E. C. Souza, et al., "Analytical and experimental modeling and simulation of a magnetic braking system for pipeline oil applications," *IEEE Transactions on Magnetics*, Vol. 50, No. 11, 8600404, 2014.

22. Jin, J. and J. Wang, *Electromagnetic Field Finite Element Method*, Xi'an University of Electronic Technology Press, Xi'an, 1998.

23. Zhang, Y., J. Ruan, T. Huang, et al., "Calculation of temperature rise in air-cooled induction motors through 3-D coupled electromagnetic fluid-dynamical and thermal finite-element analysis," *IEEE Trans. Magn.*, Vol. 48, 1047–1050, 2012.

24. Eteiba, M. B., M. M. A. Aziz, and J. H. Shazly, "Heat conduction problems in SF6 gas cooled-insulated power transformers solved by the finite-element method," *IEEE Trans. Power Del.*, Vol. 23, 1457–1463, 2008.

25. Panton, R. L., *Incompressible Flow*, 4th edition, Wiley, North America, 2013.

26. Incropera, F. P., A. S. Lavine, T. L. Bergman, et al., *Fundamentals of Heat and Mass Transfer*, Wiley, 2007.

27. Xiao, C., K. Wei, D. Cheng, et al., "Wireless charging system considering eddy current in cardiac pacemaker shell: Theoretical modeling, experiments, and safety simulations," *IEEE Trans. Ind. Electron.*, Vol. 64, 3978–3988, 2016.

28. Chen, W., X. Huang, W. Sun, et al., "Influence of metal obstacles on magnetically coupled resonant radio energy transmission system," *Journal of Electrotechnics*, Vol. 29, 22–26, 2014.

29. Yang, Q., P. Zhang, L. Zhu, et al., "Key basic and technical bottlenecks of radio energy transmission technology," *Journal of Electrotechnics*, Vol. 30, 1–8, 2015.

30. Bian, Y., Y. Sun, X. Dai, et al., "Modeling and analysis of magnetic energy mode radio energy transmission system," *Proc. Chin. Soc. Electrical Eng.*, Vol. 32, 155–160, 2012.

31. Gowrishankar, T. R., D. A. Stewart, G. T. Martin, et al., "Transport lattice models of heat transport in skin with spatially heterogeneous," *Temperature-dependent Perfusion Biomed. Eng. Online*, Vol. 3, 42, 2004.